Finite Element Analysis of Aluminium Alloy and Carbon-Fibre-Reinforced ABS Conveyor Idler Roller Materials

Abraham Foiebi Oyoko and Anthony Chijioke Adingwupu*

Department of Mechanical Engineering, Igbinedion University, Okada, Edo State Nigeria.
*Corresponding Author's Email: abraham.foiebi@iuokada.edu.ng, Anthony.adingwupu@iuokada.edu.ng

Direct Research Journal of Engineering and Information Technology

Vol. 14(1), Pp. 139-149, April 2026,
Author(s) retain the copyright of this article
This article is published under the terms of the Creative Commons Attribution License 4.0.
Research Article
ISSN: 2354-4155
https://journals.directresearchpublisher.org/index.php/drjeit; https://www.ajol.info/index.php/drjeit

Received 17 January 2026, Accepted 5 April 2026, Published 30 April 2026

ABSTRACT

This study presents a finite element analysis of aluminium alloy and carbon-fibre-reinforced Acrylonitrile Butadiene Styrene (CF-ABS) materials for conveyor idler roller applications. A flat type idler roller was designed in accordance with CEMA standards and modelled using SolidWorks, while structural simulations were conducted in ANSYS Workbench under static loading conditions. The performance of aluminium alloy was compared with CF ABS composites containing varying carbon fibre contents (70%, 80%, and 90%). Key response parameters including total deformation, von Mises stress, strain, and bearing reaction forces were evaluated under trough angles ranging from 0° to 60°. Results showed that aluminium alloy exhibited the lowest deformation (8.40×10^{-5} m), while CF ABS composites recorded higher deformation values between 2.61×10^{-3} m and 3.24×10^{-3} m depending on fibre content. However, stress levels in CF ABS increased with fibre proportion, reaching up to 8.43 × 106 Pa at 90% carbon fibre content. Bearing reaction forces remained nearly constant at approximately 2538.7 N across all cases, indicating independence from material variation and trough angle. CF-ABS composites therefore demonstrated a favourable balance between lightweight characteristics and acceptable mechanical performance, suggesting their potential as sustainable alternatives to aluminium alloy in conveyor idler roller design.

Keywords: *Aluminium alloy, ANSYS simulation, Carbon-fibre-reinforced ABS, Composite materials, Conveyor idler roller, Finite element analysis*

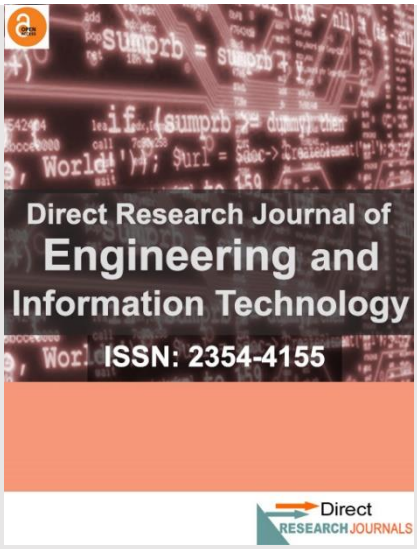

Citation: Oyoko, A. F. & Adingwupu, A. C. (2026). Finite Element Analysis of Aluminium Alloy and Carbon-Fibre-Reinforced ABS Conveyor Idler Roller Materials. *Direct Research Journal of Engineering and Information Technology*, 14(1), Pp. 139-149. https://doi.org/10.26765/DRJEIT009047815

INTRODUCTION

Conveyor belt systems are extensively applied in mining, manufacturing, and bulk material transport industries because they offer continuous, reliable, and energy efficient movement of materials over long distances. A fundamental element of these systems is the idler roller, which supports the conveyor belt and its load, helps maintain correct alignment, and reduces frictional resistance, thereby enabling stable and efficient operation (Lodewijks, 2020). Although idler rollers do not actively transmit power, they have a direct influence on conveyor performance, energy demand, maintenance frequency, and overall system reliability. In service, idler rollers are exposed to repeat cyclic loading caused by belt tension, material weight, and dynamic effects within the conveyor system. These operational conditions can trigger several failure mechanisms such as fatigue damage, bearing degradation, excessive vibration, and misalignment. Over time, these issues increase power consumption, shorten component lifespan, and may result in unexpected downtime (Qiu et al., 2021; Adingwupu *et al.* 2020). For this reason, both the structural design and material selection of idler rollers are critical considerations in conveyor engineering. Aluminium alloys are commonly adopted for idler roller construction because they provide a favourable balance between strength and weight, as well as good resistance to corrosion. However, despite these advantages, aluminium-based components still present important limitations, including relatively high material density, reduced vibration absorption capability, and substantial environmental burdens linked to energy intensive extraction and refining processes. The production of aluminium is particularly associated with high greenhouse gas emissions, making its long-term sustainability a concern in modern engineering applications (Habashi, 2020). In broader life cycle studies, metallic materials are consistently reported to have higher embodied energy compared with many polymer-based alternatives (European Commission, 2010).

Driven by increasing emphasis on sustainable engineering practices, attention has shifted toward lightweight materials capable of maintaining adequate mechanical performance while reducing environmental impact. In this context, the strength-to-weight ratio is a key material selection criterion because it reflects the ability of a material to withstand applied loads with minimal mass contribution, thereby improving energy efficiency in dynamic systems (Ashby, 2011). In conveyor applications, reducing component mass can lower rolling resistance and decrease the load imposed on bearings and drive systems. Polymer matrix composites reinforced with carbon fibres have emerged as strong candidates for replacing conventional metals in structural applications. These materials offer high specific strength, corrosion resistance, and considerable design adaptability (Mallick, 2021). In particular, carbon-fibre-reinforced Acrylonitrile Butadiene Styrene (CF-ABS) has gained interest due to its manufacturability using modern processes, improved mechanical performance compared to neat polymers, and potential for reduced life cycle environmental impact. Experimental investigations have shown that CF-ABS composites demonstrate enhanced stiffness and load-bearing capability relative to unreinforced ABS, making them suitable for engineering components subjected to moderate structural loads (Karupaiah & Narayanan, 2022). Despite these promising attributes, the application of CF-ABS composites in conveyor idler rollers remains limited in the literature, particularly regarding their behaviour under realistic loading conditions, such as varying trough angles and bearing constraints. In addition, the environmental performance of such composites is strongly dependent on fibre content and manufacturing processes, which necessitates a careful balance between reinforcement level, mechanical performance, and sustainability outcomes.

This study therefore investigates and compares the mechanical behaviour of aluminium alloy and carbon-fibre-reinforced ABS composites for conveyor idler roller applications. A standard flat-type idler roller geometry is developed in accordance with industrial design guidelines, and Finite Element Analysis (FEA) is used to evaluate deformation, stress distribution, and bearing reaction forces under different loading conditions and trough angles. Idlers are prone to damage through the impacts of vibration, jamming and fatigue that may lead to accidents, additional energy consumption, and fire (Liu *et al*., 2023). This may lead to breakdown maintenance operations and increased production costs. This study presents the design and simulation techniques that were employed to investigate the suitability of carbon fibre nylon composite and aluminium for the production of conveyor idler rollers.

MATERIALS AND METHODS

The conceptualised conveyor idler for this study is the flat type which is based on existing types. The common ones in the industry are the impact, carrying of flat and return idlers (Loureiro et al., 2015). No matter the configuration, the impact and carrying idlers consist of three rollers in series, that rotate about a shaft. The middle roller is always horizontal and parallel to the belt, while the side rollers are positioned at an angle. The middle roller absorbs 50 to 70% of the total load (Soni and Patel, 2014).

Conveyor Idler Design

The design of the flat idler roller is presented in this section. The outer roller diameter and load were taken as 5 inches (127 mm) and 500 N according to CEMA (2005), this belongs to the class C5 of idler rollers.

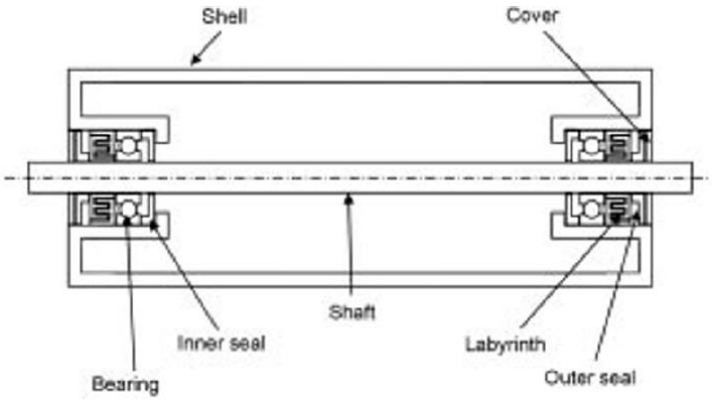

Figure 1: Illustration of the section of a conveyor idler (Yardley and Stace, 2008)

Table 1: Design parameters of the conveyor idler

S/N	Parameter	Value
1	Outer diameter	127 mm
2	Inner diameter	117 mm
3	Thickness	5 mm
4	Roller length	650 mm
5	Bearing to bearing distance	590 mm
6	Bearing size	20 mm bore, outer diameter of 42 mm
7	Shaft size	20 mm
8	Bearing centre distance from roller end	30 mm

This represents an idler that is recommended for medium duty work. A typical conveyor idler's cross-section is shown in (Figure 1). The roller is connected to its shaft by the bearing.

Design parameters

The design parameters are given in (Table 1). They include the material type and values for outer diameter, inner diameter, wall thickness, the toller length, belt width, load and the rotational speed. Some of these parameters are calculated and their respective equations are given in details. The design is based on the general guidelines of DIN, CEMA and ANSI (Yardley and Stace, 2008).

The inner diameter was calculated according to Equation 1.

$$D_i = D_o - 2t \quad (1)$$

The roller length is the addition of the belt length and clearance size on the left and right sides of the belt. This is presented in Equation 2.

$$R_l = B_l + 2c \quad (2)$$

B_l is the belt length (500 mm) and c is the belt clearance (75 mm).

The bearing was placed close to the roller ends to minimize bending stress on the shaft. Therefore, the bearing centres are 30 mm from each end and the bearing-to-bearing distance is 590 mm. Using the applied load (W) and the roller length, L, the bending moment of the roller was calculated based on Equation 3/

$$M = \frac{WL}{2} \quad (3)$$

The section modulus of the shaft is a function of the bending moment and can be determined using Equation 4.

$$Z = \frac{M}{\sigma} \quad (4)$$

The length and diameter of the shaft were also calculated using equations 5 and 6.

$$S_l = R_l + 2c \quad (5)$$

$$d = \left(\frac{32M}{\sigma\pi}\right)^{1/3} \quad (6)$$

Geometric Modelling of the Idler

The calculated idler and shaft parameters are used to develop the geometry. The geometry modelling was done in SolidWorks and the front, side, top and isometric views are shown in (Figure 2).

Material Properties

The materials used for this study are Aluminium alloy and Acrylonitrile Butadiene Styrene (ABS) matrix with carbon-fibre. The simulations of these materials were done

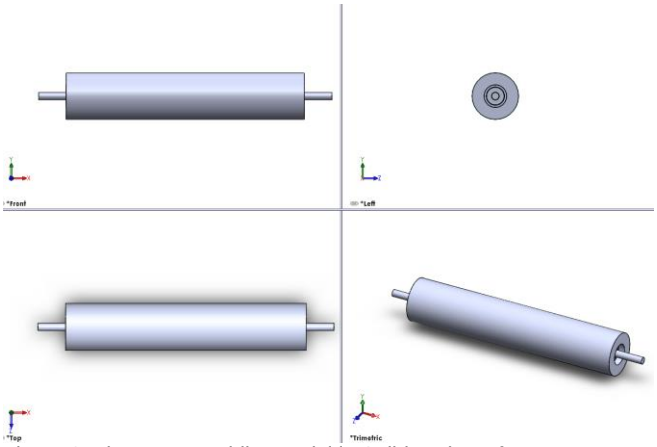

Figure 2: The conveyor idler model in SolidWorks software

separately. The amount of carbon-fibre that was added to ABS is 10, 20 and 30%, and the variation is to test its effect on the mechanical properties of the idler roller made with composite material.

The rule of mixtures was applied to determine the effective properties of the composites. For the density, Equation (7) was used.

$$\rho_{composite} = v_{cf}\rho_{cf} + v_{ABS}\rho_{ABS} \quad (7)$$

Similarly, the Young's modulus in of the composite material can be calculated based on Equation (8).

$$E_{effective} = v_{cf}E_{cf} + v_{ABS}E_{ABS} \quad (8)$$

$$G_{effective} = \frac{G_{cf}G_{ABS}}{v_{cf}G_{ABS} + v_{ABS}G_{cf}} \quad (9)$$

$$v_{effective} = v_{cf}v_{cf} + v_{ABS}v_{ABS} \quad (10)$$

The material data for the properties were obtained from ANSYS material libraries except for the tensile ultimate strength of carbon fibre which is not included in the available properties. Also, carbon fibre does not have a defined tensile yield strength because of its brittle nature (Langston, 2016; Ajayi & Adingwupu, 2014). Based on this condition, the tensile yield strength of carbon fibre was taken as zero. The tensile ultimate strength data for carbon fibre was taken from Gu et al. (2015). The ultimate tensile strength was calculated using Equation (11) while the effective tensile yield strength was computed with Equation (12).

$$\sigma_{effective} = v_{cf}\sigma_{cf} + v_{ABS}\sigma_{ABS} \quad (11)$$

$$\sigma_{yield,\ comp} = v_{cf}\sigma_{yield,\ cf} + v_{ABS}\sigma_{yield\ ABS} \quad (12)$$

The properties of Aluminium alloy were obtained directly from ANSYS material library. An extract from inside the

Density	2770 kg/m³
Young's Modulus	7.1e+10 Pa
Thermal Conductivity	table(T) = 148.62 W/m·°C
Specific Heat	875 J/kg·°C
Tensile Yield Strength	2.8e+08 Pa
Tensile Ultimate Strength	3.1e+08 Pa

Figure 3 Properties of Aluminium alloy

ANSYS Static Structural Package showing the properties of Aluminium alloy is shown in (Figure 3).

Finite Element Analysis

The Finite Element Method (FEM) is one of the numerical techniques that are used to find approximate solutions to differential equations that govern physical problems. The FEM is commonly employed to solve problems involving solid objects or structural bodies. To use the FEM in ANSYS, the Structural package is used to model and define the physical problem. The steps taken to perform this task and accomplish a complete solution are generally categorised into three: (i) pre-processing, (ii) processing, and (iii) post processing. The procedures taken in each step are described in the following sections.

The first thing is to create a project in the ANSYS 2022 R1 Workbench window and stating a new Static Structural Project. The solution container in ANSYS workbench is presented in (Figure 4).

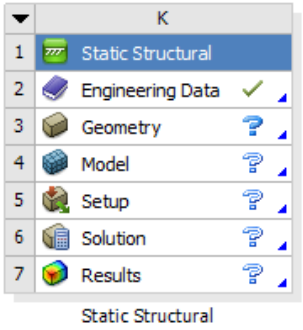

Figure 4: The Static Structural application in ANSYS workbench

In Figure 4, each row represents the stage of solution. Engineering data is where materials that are required for the project are selected or defined. The materials that are not available in the material library can be created based on their properties. All the materials required for this project were defined and selected at this stage. The next stage is the geometry interface which is controlled by SpaceClaim modelling software. The geometry created in SolidWorks was imported into SpaceClaim and this can be seen in Figure 5 (a). The parts that are not required in the FEM simulations such as the shaft and bearings are excluded from the geometry. The cleaned-up geometry is presented in Figure 5 (b). Named selections that are used for assigning boundary conditions during the setup

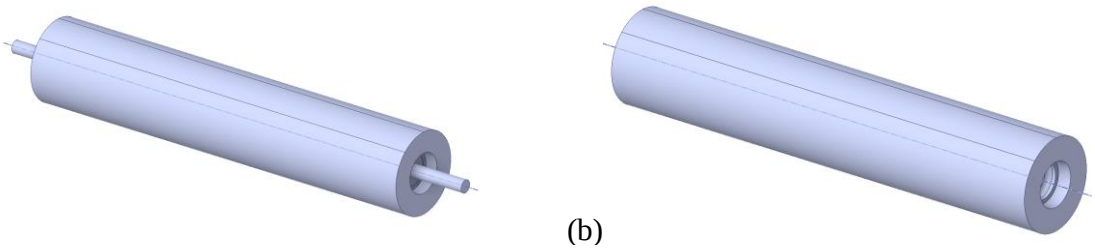

(a) (b)

Figure 5: ANSYS Spaceclaim view (a) after importation of the geometry made in SolidWorks, (b) after clean-up of the geometry.

stage are also created. The two named selections created for this study are belt and bearings. The belt named selection represented the area of the roller that is in contact with the belt while bearings represent the parts of the idler that are supported by bearings. After the geometry has been appropriately prepare, meshing is performed to divide the computational object into discrete forms. The next stage is the setup, which involves (i) assigning the material to the geometry, (ii) assigning loads, and (iv) creating solution types.

Processing

This stage involves solving the mathematical model of the FEM. Computer resources are required to provide the solution which depends on the those created during the pre-processing stage. The solutions include deformation, Von Mises strain and stress and reactions forces developed at the bearings. The solutions obtained after the processing stage are visualised and interpreted. The complete solution tree is presented in (Figure 6).

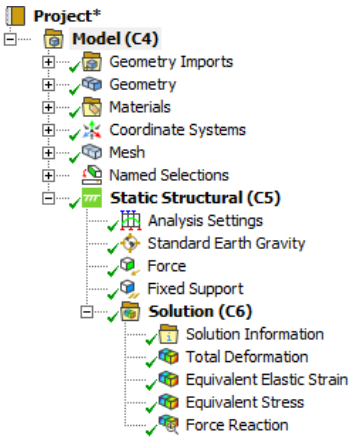

Figure 6: The solution tree of the FEM model

Boundary Conditions

The force exerted on the conveyor roller is based on the findings of (Bombasaro and Oddera, 2021). The following boundary conditions were used for the simulation:

i. A force of 2000 N acts on the area of the roller that makes contact with the belt.
ii. Frictionless support at the bearings.
iii. The trough angle of the idler was varied from 0° to 60° based on conventional idler designs (Figures 7a-c). This has implications on the direction of the acceleration due to gravity. In the modelling setup, the direction of *g* was varied as 0°, 15°, 30°, 45° and 60°, corresponding to the through angles.
iv. The angle of contact is taken as 24° and the load on the idler is assumed to be uniformly distributed. Mesh

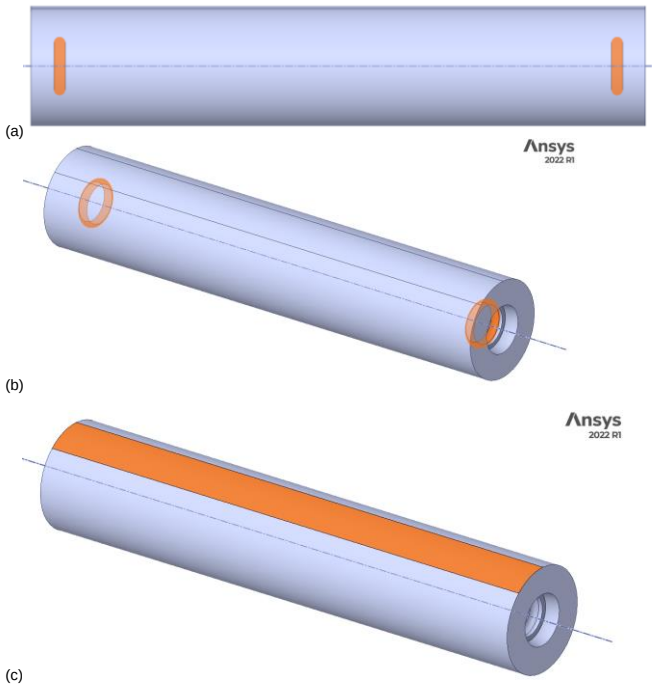

Figure 7: (a) Front view of the idler showing the location of the bearing boundary conditions, (b) the isometric view of the conveyor idler showing the locations of the bearings, and (c) illustration of the area of the idler pulley that makes contact with the belt with an angle of 24°.

Four meshes of various refinements were generated for the problem. Table 2 shows the various meshes and their

Table 2: Details of meshes used for the grid independence test

Mesh	Refinement Level	Number of Nodes	Number of Elements
1	0	17,853	9,638
2	1	62,117	31,107
3	2	143,365	74,054
4	3	246,564	123,978

descriptions. This is to allow for a grid independence test that shows that the solution does not vary significantly across various mesh sizes. The first mesh has 17,853 nodes and 9,638 elements. The mesh is shown in (Figure 8), it is coarse and without any refinement. The coarse grid is presented in (Figure 8) Level one refinement was applied in ANSYS meshing to give the second mesh which consists of 62,117 nodes and 31,107 elements. The third mesh has level two refinements and consists of 143,365 nodes and 74,054 elements. The isometric view of the mesh is shown in (Figure 9). The fourth mesh has number of elements as 246,564 and 123,978, respectively.

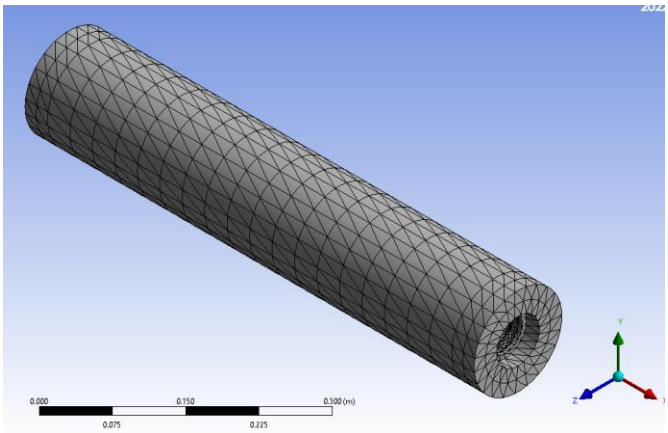

Figure 8: The coarse mesh used for the grid independence test

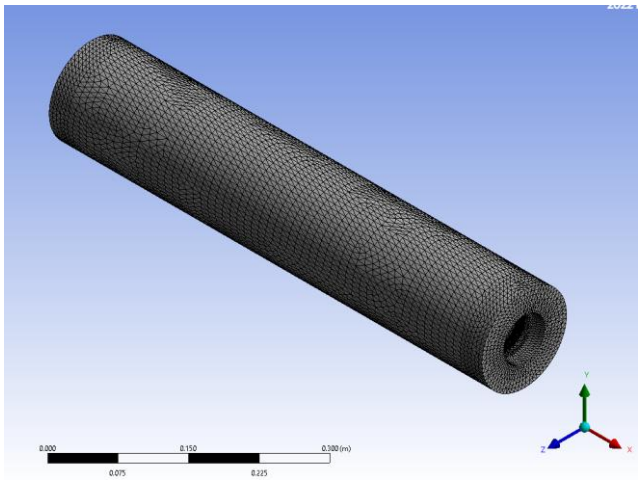

Figure 9: The mesh with refinement level 2 that was used for the grid independence test

RESULTS AND DISCUSSION

Grid Independence Test

The result of the grid independence test is summarized in (Table 3). Aluminium alloy was used as the idler material and the respective boundary conditions were applied. The direction of the applied force is shown in (Figure 10).

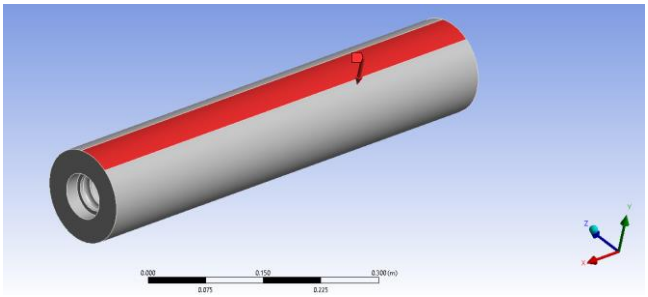

Figure 10 : The direction and location of the distributed force applied on the idler pulley

Using a simulation time of 1 s, the force of reaction obtained at the bearings for all the meshes were the same with a value of 2,538.7 N. The deformation increased with the number of nodes but the differences between the values were less than 1%. The same trend was observed for other parameters such as the maximum equivalent stress and maximum equivalent strain. Since the differences in results are small, the mesh independence test is positive and has revealed that there is little variation in the changes in values obtained in the results for total deformation, maximum equivalent strain and maximum equivalent stress. There is no difference in the reaction forces. Considering that computational time and resources increase with the number of elements and nodes of the mesh, the third mesh was chosen for the simulations performed in this project. The results obtained are certain to be reliable because of this verification.

Effect of Idler Material on Idler Deformation, Stress and Bearing Reaction

The effect of the material used for the fabrication of the idler roller on the deformation, stress and bearing reactions was studied. The first material is aluminium alloy. This is a common material that is used for the manufacturing of idler pulleys. The other samples are the composites of carbon fibre and ABS. The samples are presented in (Table 4).

Based on samples A to D, the calculated material properties are given alongside that of aluminium alloy in (Table 5). The properties were assigned through the Engineering Data interface of ANSYS Static Structural.

The contours that show the total deformation, Von Mises strain and stress of the idler material are presented in (Figure 11).

Table 3: Summary of the result of the mesh independence test

Mesh	Total Deformation (m)	Maximum Equivalent Strain (m/m)	Maximum Equivalent Stress (Pa)	Force of Reaction (N)
1	7.8581e-005	1.2358e-004	8.7309e+006	2538.7
2	8.3656e-005	1.2936e-004	9.1837e+006	2538.7
3	8.4039e-005	1.3085e-004	9.2905e+006	2538.7
4	8.4085e-005	1.3202e-004	9.3733e+006	2538.7

Table 4: The material samples considered for the conveyor idler roller

Samples	Combinations		
	Aluminium Alloy	Carbin Fibre (290 GPa)	ABS (High-impact)
A	100%	0	0
B	0	70%	30%
C	0	80%	20%
D	0	90%	10%

Table 5: Properties of aluminium alloy (sample A) and calculated effective properties for samples B, C and D

Properties	Samples			
	A	B	C	D
Density (kg/m^3)	2,770	1,216	1,184	1,107
Young's Modulus (Pa)	7.1E+10	2.26E+09	2.00E+09	1.79E+09
Shear Modulus (Pa)	2.6692E+10	8.3938E+08	7.11E+08	6.4481E+08
Poisson Ratio	0.33	0.34623	0.36712	0.38801
Tensile Ultimate Strength (Pa)	3.1e+08	3.93E+09	4.49E+09	5.04E+09
Tensile Yield Strength (Pa)	2.8e+08	8.23E+06	5.49E+06	2.74E+06

Table 6: The maximum deformation, Von Mises strain, Von Mises stress and reaction force for the various samples when the idler is perfectly horizontal.

Samples	Parameters			
	Maximum Total Deformation (m)	Maximum Equivalent Strain (m/m) per unit mass	Maximum Equivalent Stress (Pa) per unit mass	Total Reaction Force at the Bearings (N)
A	8.4039e-005	3.37E-05	2.40E+06	2538.7
B	2.6146e-003	2.30E-03	5.21E+06	2517
C	2.9299e-003	2.74E-03	5.48E+06	2516.5
D	3.2439e-003	3.24E-03	5.80E+06	2515.5

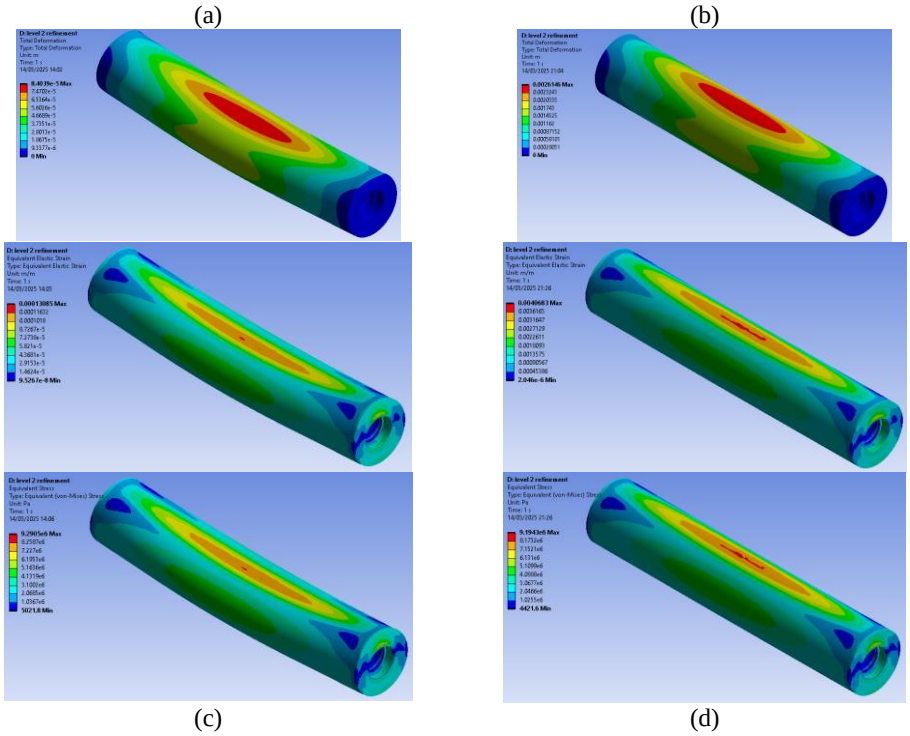

Figure 11: Deformation, Von Mises Strain, and Von Mises Stress for samples (a) A, (b) B, (c) C, and (d) D.

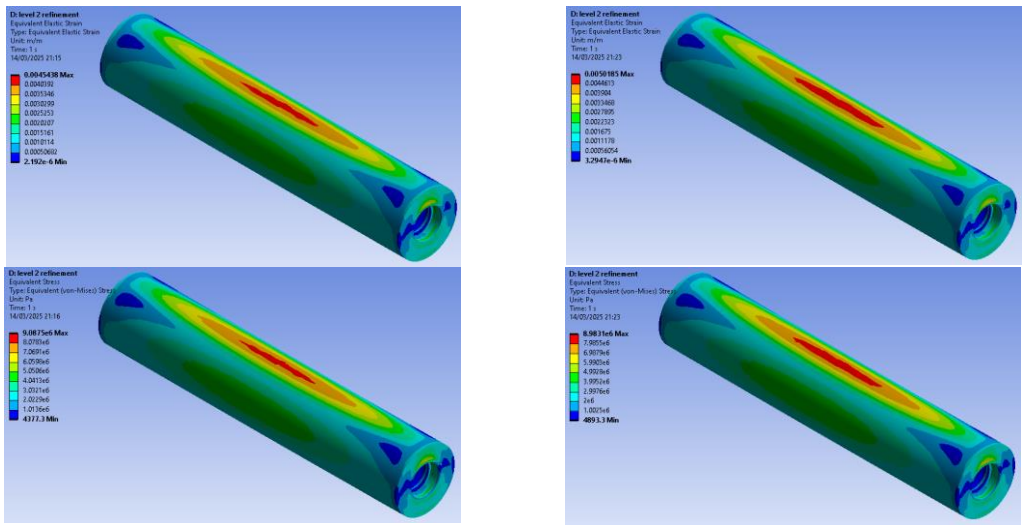

Figure 11: Deformation, Von Mises Strain, and Von Mises Stress for samples (a) A, (b) B, (c) C, and (d) D.

Table 7: The maximum deformation, Von Mises strain, Von Mises stress and reaction force for the various samples when the trough angle of the idler is 15°.

Samples	Parameters for 15° Trough Angle			
	Maximum Total Deformation (m)	Maximum Equivalent Strain (m/m) per unit mass	Maximum Equivalent Stress (Pa) per unit mass	Total Reaction Force at the Bearings (N)
A	8.1358e-005	3.53E-05	2.50E+06	2538.7
B	2.5311e-003	2.44E-03	5.49E+06	2517
C	2.8364e-003	2.96E-03	5.91E+06	2516.5
D	3.1403e-003	3.58E-03	6.39E+06	2515.5

The deformation and stresses are concentrated close to the centres of the idler. This is because of the force being applied by the load and the weight of the belt on the top side of the idler roller. The ends are less deformed due to the reactions of the bearings. The deformation and stresses also reduce towards the bottom sides of the idlers. The figure also shows that the strains and stresses are more distributed than total deformation. The contours are similar to those obtained in FEM simulation studies for stress analysis such as Wheatley and Zaeimi (2021) and Nangare and Sonawane (2022).

The values of maximum deformation, Von Mises strain per unit mass, Von Mises stress and strain per unit mass and reactions are reported in (Table 6). Sample A had the lowest deformation while Sample D had the highest. In a similar way,

Sample A and D had the lowest stress and highest stress per unit mass, respectively. This shows that Sample A is more rigid due to higher strength per unit mass while sample D is more flexible. The results also show that based on samples B, C and D, the strength per unit mass increased as the amount of carbon fibre in ABS increased. The total reactions at the bearings also increased with the strength to mass ratio. For lower strength materials, the deformation of the idler absorbs part of the force and reduce the reactions at the bearings. While this may result in misalignment, it can also increase bearing life as less load acts on it (Zhang et al., 2020). The lower strength to mass ratio can be attributed to weak fibre-matrix interfacial bonding produced by an insufficient proportion of fibres content in the matrix (Oudah et al., 2021).

Effect of Trough Angle on Idler Deformation, Stress and Bearing Reaction

The effect of the bearing trough angle on the mechanical performance of the conveyor idler roller was also examined. Figure 12 shows idler rollers with trough angle of 30°. Figure 12(a) shows that the force now acts at an angle to the surface normal and Figure 12(b) shows that the direction of gravitational pull. The cases considered are trough angles of 15°, 30°, 45°, and 60°.The 3-dimensional contours of the deformation obtained for Sample A and C for horizontal trough angle, 30° and 60° are shown in (Figure 13). It was observed that the distributions of deformation extended more to the upper part of the idler and it increased with increase in trough angle. The deformation at the sides of the idler rollers also increased. The result give insight to the positioning of rollers at the sides of the conveyor idler assembly.

Tables 7 to 10 show the maximum total deformation and other parameters that were investigated in this study. It is clear that the reaction forces remain the same irrespective of the trough angle. Therefore, bearing and idler lifespan are not affected by the angle of installation

Table 8: The maximum deformation, Von Mises strain, Von Mises stress and reaction force for the various samples when the trough angle of the idler is 30°.

Samples	Parameters for 30° Trough Angle			
	Maximum Total Deformation (m)	Maximum Equivalent Strain (m/m) per unit mass	Maximum Equivalent Stress (Pa) per unit mass	Total Reaction Force at the Bearings (N)
A	7.3484e-005	4.13E-05	2.92E+06	2538.7
B	2.2859e-003	2.85E-03	6.42E+06	2517
C	2.5615e-003	3.47E-03	6.91E+06	2516.5
D	2.8358e-003	4.19E-03	7.47E+06	2515.5

Table 9: The maximum deformation, Von Mises strain, Von Mises stress and reaction force for the various samples when the trough angle of the idler is 45°.

Samples	Parameters for 45° Trough Angle			
	Maximum Total Deformation (m)	Maximum Equivalent Strain (m/m) per unit mass	Maximum Equivalent Stress (Pa) per unit mass	Total Reaction Force at the Bearings (N)
A	6.1257e-005	4.62E-05	3.01E+06	2538.7
B	1.9052e-003	3.12E-03	6.61E+06	2517
C	2.1346e-003	3.69E-03	7.11E+06	2516.5
D	2.3629e-003	4.34E-03	7.67E+06	2515.5

Table 10: The maximum deformation, Von Mises strain, Von Mises stress and reaction force for the various samples when the trough angle of the idler is 60°.

Samples	Parameters for 60° Trough Angle			
	Maximum Total Deformation (m)	Maximum Equivalent Strain (m/m) per unit mass	Maximum Equivalent Stress (Pa) per unit mass	Total Reaction Force at the Bearings (N)
A	4.5776e-005	4.68E-05	3.29E+06	2538.7
B	1.4229e-003	3.23E-03	7.23E+06	2517
C	1.5938e-003	3.93E-03	7.79E+06	2516.5
D	1.7637e-003	4.75E-03	8.43E+06	2515.5

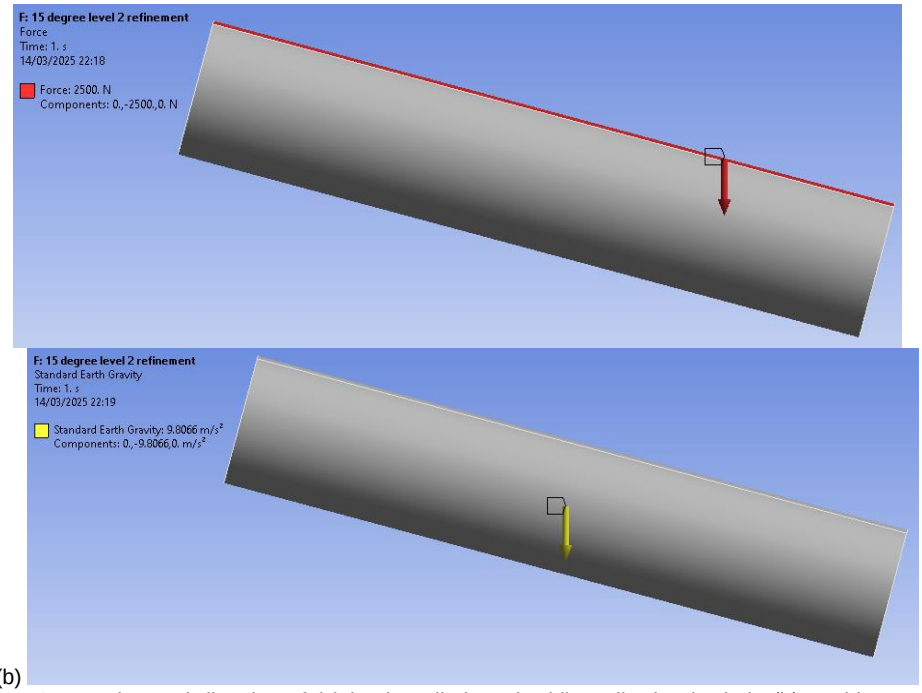

(b)

Figure 12: Location and direction of (a) load applied on the idler roller by the belt, (b) earth's gravitational force.

of the conveyor idlers. The pattern of the results of the angled idlers for maximum deformation and Von Mises strain and stress per unit mass show that it is consistent with the case of horizontal idlers. Generally, the values reduce with increasing trough angle.

The result agrees with the findings of Human and Neil (2011) that reported higher load bearing capacities as trough angles increase.

Sample A, 0° trough angle

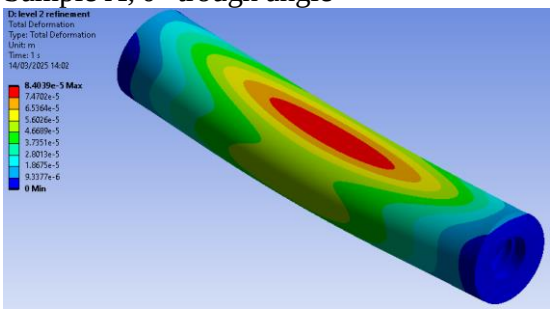

Sample C, 0° trough angle

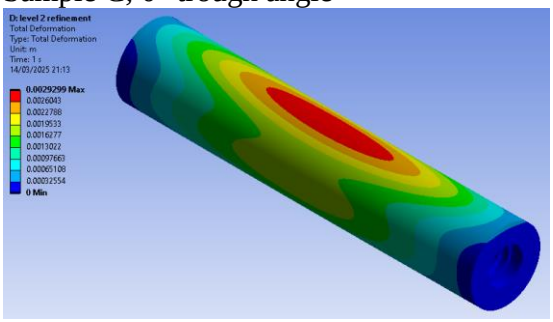

Sample A, 30° trough angle

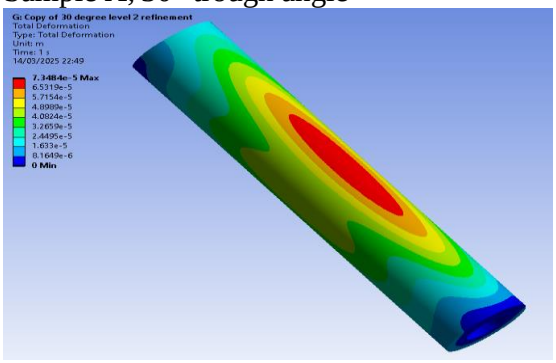

Sample C, 30° trough angle

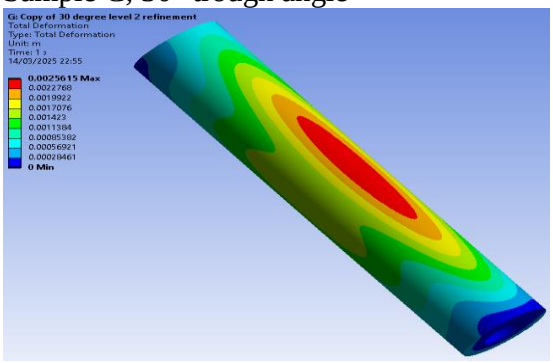

Sample A, 60° trough angle

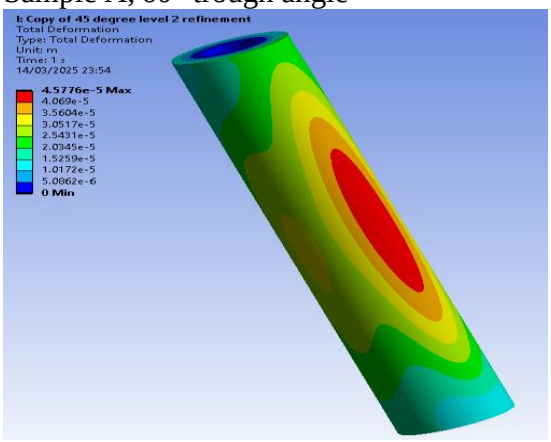

Sample A, 60° trough angle

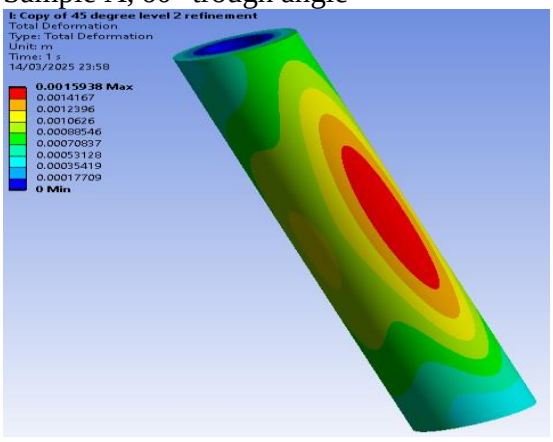

Figure 13: Contours of total deformation, Von Mises strain and Von Mises stress for various trough angles.

Conclusion

This study presented a finite element investigation of aluminium alloy and carbon-fibre-reinforced ABS (CF-ABS) materials for conveyor idler roller applications under varying trough angles. The results demonstrated that aluminium alloy exhibited significantly lower deformation (8.40×10^{-5} m) compared to CF-ABS composites (ranging from 2.61×10^{-3} m to 3.24×10^{-3} m), indicating higher stiffness but also greater sensitivity to mass related structural loading. Conversely, CF-ABS composites showed higher deformation but maintained acceptable stress distribution, with maximum von Mises stress values increasing from 5.21×10^{6} Pa to 5.80×10^{6} Pa as carbon fibre content increased from 70% to 90%. The analysis further revealed that bearing reaction forces remained nearly constant across all materials and trough angles at approximately 2538.7 N, indicating that support reactions are largely independent of material selection and geometric inclination. Increasing trough angle from

0° to 60° resulted in a reduction in total deformation for all materials, with aluminium decreasing from 8.40×10^{-5} m to 4.58×10^{-5} m and CF ABS composites showing a similar decreasing trend, confirming improved structural stability at higher trough angles. The results indicate that while aluminium alloy provides superior rigidity, CF ABS composites offer a favourable balance between reduced density and adequate mechanical performance, particularly when optimized fibre content is used. Therefore, CF ABS materials present a viable lightweight alternative for conveyor idler rollers, with potential benefits in weight reduction and system efficiency.

REFERENCES

Adingwupu A. C., Oluwafemi J. D. and Emifoniye E. U; (2020) Numerical Modeling of Food Waste Pellet Gasification Through a Downdraft Gasifier, Journal of the Nigerian Association of Mathematical Physics, Vol 56, pp105 – 110

Ajayi, K. T and Adingwupu, A**.** (2014) Mathematical Modeling of Pumps in Multiple Connections. Research Journal in Engineering and Applied Sciences 3(6) 423-432

Ashby, M. F. (2011). *Materials selection in mechanical design* (4th ed.). Butterworth-Heinemann.

Bombasaro, E., & Oddera, R. (2021). Field measurement of contact forces on rollers for a large diameter pipe conveyor. Open Engineering, 11(1). https://doi.org/10.1515/eng-2021-0014

CEMA, C. E. M. A. (2005). Belt Conveyors for Materials Handling (6th ed.).

Gu, H. X., Wang, H. J., & Fan, L. D. (2015). Structure Characterization and Property Analysis of HKT800 Carbon Fiber. Applied Mechanics and Materials, 799–800. https://doi.org/10.4028/www.scientific.net/amm.799-800.183

European Commission. (2010). *International reference life cycle data system (ILCD) handbook: General guide for life cycle assessment—Detailed guidance*. Publications Office of the European Union.

Habashi, F. (2020). Energy consumption and environmental impact of aluminum production. *Journal of Sustainable Metallurgy, 6*(4), 470–480. https://doi.org/10.1007/s40831-020-00327-9

Karupaiah, V., & Narayanan, V. (2022). Quasi-static and dynamic mechanical analysis of carbon-fibre-reinforced ABS composites. *Materiale Plastice, 59*(3), 45–56. https://doi.org/10.37358/MP.22.3.5613

Langston, T. (2016). The tensile behavior of high-strength carbon fibers. Microscopy and Microanalysis, 22(4). https://doi.org/10.1017/S143192761601134X

Lodewijks, G. (2020). Energy efficiency and reliability of belt conveyor systems. *Bulk Solids Handling, 40*(3), 38–45.

Liu, Y., Miao, C., Li, X., Ji, J., Meng, D., & Wang, Y. (2023). A Dynamic Self-Attention-Based Fault Diagnosis Method for Belt Conveyor Idlers. Machines, 11(2). https://doi.org/10.3390/machines11020216

Loureiro I.E.E., Cousseau T., da Silva C.H., & Pacholok D.E. (2015). Design Optimization, Analysis And Remedies Over Failure Of Charging Belt Conveyor System Used In The Industry To Set The Optimum Results. International Journal of Advance Engineering and Research Development, 2(03). https://doi.org/10.21090/ijaerd.020359

Mallick, P. K. (2021). *Fiber-reinforced composites: Materials, manufacturing, and design* (4th ed.). CRC Press.

Nangare, V. A., & Sonawane, D. P. R. (2022). Design, Analysis and Weight Optimization of Roller Conveyor System by using Glass Fiber Composite Material. International Journal for Research in Applied Science and Engineering Technology, 10(7). https://doi.org/10.22214/ijraset.2022.45569

Soni, H. J., & Patel, R. R. (2014). Design and Optimization of Idler for Belt Conveyor. International Journal for Scientific Research & Development, 2(4), 222–227.

Qiu, M., Wang, X., & Chen, Z. (2021). Dynamic response and vibration characteristics of conveyor rollers. *Mechanical Systems and Signal Processing, 154*, 107547. https://doi.org/10.1016/j.ymssp.2020.107547

Wheatley, G., & Zaeimi, M. (2021). Composite shaftless roller design for conveyor system. Periodica Polytechnica Mechanical Engineering, 65(3). https://doi.org/10.3311/PPme.17554

Yardley, E. D., & Stace, L. R. (2008). *Bulk solids handling: An introduction to the practice and technology*. Springer.

Zhang, Y., Zhang, M., Wang, Y., & Xie, L. (2020). Fatigue life analysis of ball bearings and a shaft system considering the combined bearing preload and angular misalignment. Applied Sciences (Switzerland), 10(8). https://doi.org/10.3390/APP1008275